Theor Chem Acc (1998) 99:158–165

Theoretical
Chemistry Accounts

Regular article

Inclusion of exact exchange for self-interaction corrected H_3 density functional potential energy surface

Gabor I. Csonka[1], **Benny G. Johnson**[2]

[1] Department of Inorganic Chemistry, Technical University of Budapest, H-1521 Budapest, Hungary
[2] Q-Chem Inc., 317 Whipple Street, Pittsburgh, PA 15218, USA

Received: 13 August 1997 / Accepted: 14 November 1997

Abstract. The effect of the inclusion of the exact exchange into self-interaction corrected generalized gradient approximation density functional theory (GGA-DFT) for the simplest hydrogen abstraction reaction, $H + H_2 \rightarrow H_3 \rightarrow H_2 + H$, is presented using a triple-zeta augmented 6-311++G(*d*,3*pd*) basis set. The introduction of the self-interaction correction has a considerably larger effect on molecular geometry and vibrational frequencies than the inclusion of the exact exchange. We investigate the influence of the self-interaction error on the shape of the potential energy surface around the transition state of the hydrogen abstraction reaction. The decomposition of the self-interaction error into correlation and exchange parts shows that the exchange self-interaction error is the main component of the energy barrier error. The best agreements with the experimental barrier height were achieved by self-interaction corrected B3LYP, B-LYP and B3PW functionals with errors of 1.5, 2.9 and 3.0 kcal/mol, respectively.

Key words: Hydrogen abstraction reaction barrier – Self-interaction components – B3LYP and B3PW functionals – Self-interaction corrected molecular geometries – Self-interaction corrected total energies

1 Introduction

In this paper we present the effect of the inclusion of the exact exchange into self-interaction corrected density functional theory (DFT) for the simplest hydrogen abstraction reaction, $H + H_2 \rightarrow H_3 \rightarrow H_2 + H$. This reaction is of fundamental practical and theoretical significance. The potential energy surface of this reaction was studied in detail by high-level theoretical methods [1–3] recently. The practical importance arises from the observation that the rate-limiting step in some combustion reactions is the abstraction of a hydrogen atom from saturated hydrocarbons [4, 5]. The potential energy surfaces of some steps in hydrogen abstraction were recently studied at the ab initio level [6, 7]. The kinetics of such reactions was also studied [8] using the results of potential surface studies.

The exact Kohn-Sham (KS) spin DFT [9] predicts the spin densities, $\rho\uparrow(\mathbf{r})$ and $\rho\downarrow(\mathbf{r})$; thus the total electron density $\rho(\mathbf{r}) = \rho\uparrow(\mathbf{r}) + \rho\downarrow(\mathbf{r})$, and the energy, E_{KS}, for the ground state of a system of N electrons in an external potential, $v(\mathbf{r})$ [for molecules $v(\mathbf{r})$ is the Coulomb potential of the nuclei]. The exact self-consistent KS equations [9] yield eigenfunctions and eigenvalues, ϕ_j and ε_j, formally in the same way as the HF method; however, these orbitals reflect correlation effects and yield exact electron density, $\rho(r)$. The individual eigenfunctions and eigenvalues, ϕ_j and ε_j, of the KS equations have no strict physical significance. However, for isolated systems with $v(\infty) = 0$, the highest-occupied eigenvalue, ε_{HOMO}, controls the asymptotic decay of the total physical density. Hence it can be shown that ε_{HOMO} is the negative of the exact, many-body, ionization potential (–I). In this context it is worth noting that Perdew et al. [10] showed that the exact KS potential and its ε_{HOMO} change discontinuously as the electron number N passes through an integer M. ε_{HOMO} is $-I$ for N just below M, $-(I+A)/2$ for N = M, and $-A$ for N just above M, where $-A$ is the negative of the electron affinity.

The exact KS [9] total energy, E_{KS}, is composed from the following energy terms:

$$E_{KS} = E_T + E_V + E_J + E_X + E_C \ , \qquad (1)$$

where E_T is the non-interacting kinetic energy, E_V is electron-nuclear attraction energy, E_J is the electron-electron Coulomb repulsion energy, E_X is exchange energy and E_C is the correlation energy. For a single electron system electron-electron interaction occurs, and E_J will be nonzero; this way it contains a self-interaction error. The exact E_X and E_C correct for this error, as well as they account for the remaining exchange and correlation energy. The density functional for E_C is generally not known in exact, explicit form. However, for reasons now well understood [11], $E_X + E_C$ can be approximated

Correspondence to: G. Csonka

reliably together by local spin density approximation (LSDA) [9] and generalized gradient approximation (GGA) [12–15]. The GGA-DFT provides a very efficient recovery of electron correlation compared with very expensive traditional methods. It is possible to implement this formalism similarly to the Hartree-Fock (HF) method; thus the computational cost of DFT scales similarly to that of the HF method; however, in contrast to the HF method the GGA-DFT yields good thermochemistry in a standard thermochemical test set of molecules [16].

Further studies of GGA exchange correlation holes and the adiabatic connection formula [17] have shown that the exact exchange hole is poorly represented by GGA models in molecular bonds [18, 19]. To remedy this error a simple, hybrid GGA model was proposed and the exact exchange was mixed with the GGA functionals. The weight of the exact exchange was chosen to fit the experimental thermochemical data [18, 19]. The exact exchange mixing reduces average bond energy errors from 6 kcal/mol for GGA to about 2 kcal/mol in the same thermochemical test set of molecules [18, 19]. Recent studies show that the reaction barrier heights are also improved by exact exchange mixing [20, 21]; however, further thorough investigations are necessary.

The above-mentioned density functionals for the exchange correlation provide good results for the many-electron systems, but most of them fail to be exact for one-electron system. Approximate exchange functionals result in an imperfect cancellation of the Coulomb and exchange terms. Similarly the approximate correlation functionals result in nonzero correlation self-interaction contributions with the notable exception of the LYP functional (see below). In most of physical systems the self-interaction errors of the above-mentioned approximate functionals are only a small fraction of the total energy; however they are a considerably larger fraction of the orbital energy. Thus LSDA and GGA, which miss the derivative discontinuity, effectively average over it, providing an estimate of $-(\mathrm{I}+\mathrm{A})/2$ for the $\varepsilon_{\mathrm{HOMO}}$.

To remedy the self-interaction error, Perdew and Zunger [22] proposed an orbital-based self-interaction correction (SIC) for atoms at the LSDA level. Their starting point was the fact that density functionals $E_X[\rho\uparrow(\mathbf{r}),\ \rho\downarrow(\mathbf{r})]$ and $E_C[\rho\uparrow(\mathbf{r}),\ \rho\downarrow(\mathbf{r})]$ are exactly known for the simple one-electron density. One-electron density can be written in the following way:

$$\int \rho\uparrow(\mathbf{r}) = 1 \text{ and } \rho\downarrow(\mathbf{r}) = 0 \ . \tag{2}$$

The SIC was designed to fulfil the following exact equations for any one-electron density, $\rho\uparrow(\mathbf{r})$:

$$E_X[\rho\uparrow(\mathbf{r}), 0] = -E_J[\rho\uparrow(\mathbf{r})] \ , \tag{3}$$

$$E_C[\rho\uparrow(\mathbf{r}), 0] = 0 \ , \tag{4}$$

where 0 in the bracket is the opposite spin electron density.

The approximate exchange, $E_X^{\mathrm{approx}}[\rho\uparrow,\rho\downarrow]$ and correlation, $E_C^{\mathrm{approx}}[\rho\uparrow,\rho\downarrow]$ functionals may violate Eqs. (3) and (4) for one-electron density; however by an orbital-by-orbital SIC, they can be made exactly self-interaction free:

$$E_X^{\mathrm{SIC}}[\rho\uparrow,\rho\downarrow] = E_X^{\mathrm{approx}}[\rho\uparrow,\rho\downarrow] - \sum_i \{E_J[\rho_i] + E_X^{\mathrm{approx}}[\rho_i, 0]\} \ , \tag{5}$$

$$E_C^{\mathrm{SIC}}[\rho\uparrow,\rho\downarrow] = E_C^{\mathrm{approx}}[\rho\uparrow,\rho\downarrow] - \sum_i \{E_C^{\mathrm{approx}}[\rho_i, 0]\} \ , \tag{6}$$

where the summation covers all occupied spin orbitals, $\psi_{\mathrm{i}}(\mathbf{r})$ and $\rho_{\mathrm{i}}(\mathbf{r}) = |\psi_{\mathrm{i}}(\mathbf{r})|^2$ is the orbital density. If one-electron density is introduced into Eqs. (5) and (6) we obtain $E_X^{\mathrm{SIC}} = -E_J$ and $E_C^{\mathrm{SIC}} = 0$; thus after introducing the SIC an approximate exchange correlation functional will fulfil the exact conditions, Eqs. (3) and (4). In applications to molecules the use of KS orbital densities leads to a size consistency error [22, 23]. The KS orbitals are delocalized over the whole molecule, and as the size of the system grows, the orbitals tend to be more extended and the total self-interaction correction tends toward zero. To avoid this problem, a set of localized SIC orbitals must be constructed and used instead of KS orbitals. Then these normalized orbitals are varied during the minimization, leading to equations that resemble the KS equations. However, the orbital-independent approximate exchange correlation potential is replaced by the orbital-dependent potential. Recently these equations have been applied to GGA functionals as well [2, 24]. The GGA + SIC functional is given by

$$\begin{aligned} E_{\mathrm{tot}}[\Psi_i(\mathbf{r})] = {} & \sum_i \int \Psi_i(\mathbf{r})(-\nabla^2/2 + V_{\mathrm{ext}})\Psi_i(\mathrm{r})dr \\ & + \frac{1}{2}\iint \frac{\rho(r)\rho(r')}{r-r'}drdr' + \int F_{\mathrm{xc}}[\rho(r), \nabla\rho(r)]dr \\ & - \frac{1}{2}\sum_i \iint \frac{\rho_i(r)\rho_i(r')}{r-r'}\,dr\,dr' \\ & - \sum_i \int F_{\mathrm{xc}}[\rho_i(r), \nabla\rho_i(r)]dr \ , \end{aligned} \tag{7}$$

where the first term is the sum of the noninteracting kinetic energy and electron-nuclear attraction energy, $E_T + E_V$, the second term is the electron-electron Coulomb repulsion energy, E_J, F_{xc} is exchange correlation functional and the last two terms are the orbital-dependent SIC corrections (note that the spins are not shown for brevity). This way the self-interaction error can easily be corrected. However there is no direct method of calculating the functional derivative of an orbital-dependent energy functional with respect to the density; thus the conventional KS procedure is not applicable to the SIC. Perdew and Zunger followed an HF-like procedure in which each electron moves in a different (local DFT) potential.

In 1971 [25] Lindgren used Eq. (5) for LSDA exchange. In 1981 Perdew and Zunger [22] tested Eqs. (5) and (6) on atoms as a general method for LSDA. It was typically found for KS orbital densities of an atom that each orbital self-interaction to the LSDA exchange energy is negative, each orbital self-interaction to the LSDA correlation energy is positive, and the total cor-

rection is negative. Similar calculations were performed by Chen et al. [26] and it was observed that LSDA-SIC is a much better approximation for atoms than the LSD in predicting most of the electronic properties. LSDA + SIC predicts accurate total energy and highest-occupied orbital ionization energy. It provides self-consistent bound solutions for anions. The SIC effective potential has a correct long range behavior ($-1/\mathbf{r}$) of the KS exchange-correlation potential [22, 26]. It was observed for molecules that SIC provides orbitals corresponding to bonds, and lone pairs [27]. The molecules and solids dissociate correctly in the SIC framework to separate neutral atoms, which is not always the case for LSDA or GGA. The SIC energy is nearly exact for the uniform electron gas at electron densities common in chemical bonds [28, 29]. The SIC exchange correlation hole satisfies a sum rule although the SIC exchange hole violates the negativity constraint [22, 30].

Several problems with the SIC were also observed in the literature. It can yield "false surface energies" for metals [22, 26]. The LSDA + SIC applied to molecules yields too short bond lengths and does not considerably improve or worsen molecular atomization energies [27, 31].

We note that an alternative way to solve the self-interaction problem is to implement a self-interaction free exact exchange [32] and to construct a self-interaction free and accurate correlation functional [33]. For this purpose Grabo and Gross [34] proposed recently the self-interaction free correlation-energy functional developed by Colle and Salvetti [35, 36]. This orbital-dependent functional gives correlation energies within a few percent error of exact energies using HF orbitals. The quite successful self-interaction free LYP correlation-energy functional [15] was developed from the Colle-Salvetti functional.

The aim of this paper is to continue a previous study of the simplest hydrogen abstraction reaction barrier [2] and show the working mechanism of the functional mixing proposed by Becke [18] in the self-interaction corrected GGA-DFT formalism of Perdew and Zunger [22].

2 Computational details

We employed the following combinations of the GGA-DFT functionals for the exchange correlation energy term:

1. B-P and B-PW: Becke's exchange functional [14] is combined with the correlation functionals of Perdew [12b], and Perdew-Wang [37], respectively.

2. B-LYP: Becke's exchange functional [14] is combined with the correlation functional of Lee, Yang and Parr [15].

3. B3PW is a hybrid method. It is a linear combination of various exchange and correlational functionals in the form:

$$A \cdot E_X[\text{exact}] + (1-A) \cdot E_X[S] + B \cdot \Delta E_X[B] + E_c[VWN5] + C \cdot \Delta E_c[PW] \ ,$$

where E_x[exact], $E_x[S]$ and $\Delta E_x[B]$ are the exact, Slater and Becke exchange functionals; and E_c[VWN5] and ΔE_c[PW] are the Vosko, Wilk and Nussair [38] and Perdew-Wang [37] correlation functionals, respectively.

The constants A, B, and C are those determined by Becke by fitting heats of formations ($A = 0.2$, $B = 0.72$, $C = 0.81$) [18]. Note that the Perdew-Wang functional uses Perdew's own local functional instead of the VWN5 functional [38]. Our investigation shows that this results in a negligible difference.

4. B3LYP is a hybrid method. It is a logical extension of Becke's three-parameter concept using different correlational functionals (e.g. LYP) in the form:

$$A \cdot E_X[\text{Exact}] + (1-A) \cdot E_X[S] + B \cdot E_X[B] + (1-C) \cdot E_C[VWN5] + C \cdot E_C[LYP] \ .$$

The constants A, B and C are selected to be equal to those determined by Becke for the B3PW method [18]. Note that Gaussian 94 [39] uses E_c[VWN3] and this might lead to a considerable difference (1–2 kcal/mol).

The calculations were carried out with Q-Chem [40] and Gaussian 94 [39] programs. A fine pruned grid having 75 radial shells and 302 angular points per shell that resulted in about 7000 points per atom [39] and a 6-311++G(*d*,3*pd*) [41] basis set was used in all calculations.

3 Results and discussion

3.1 Molecular geometries and vibrational analysis

Table 1 shows the optimized equilibrium distances for the H_2 molecule and the geometric parameters for the H_3 $D_{\infty h}$ transition structure. For comparison the HF, MP2, CCSD(T) and experimental results are also shown. The B-PW results differ slightly from values published in the previous study [2] and the current values are the correct values. The KS methods show good agreement with the experimental H_2 bond length and the inclusion of the exact exchange improves further this already good agreement. The situation is similar for the H_3 $D_{\infty h}$ transition structure.

Inspection of Table 1 reveals that GGA + SIC results in a too short H_2 bond length and too short interatom distances for the H_3 $D_{\infty h}$ transition structure. It seems

Table 1. Optimized H-H distance (Å) of H_2 equilibrium and H_3 $D_{\infty h}$ transition structure[a]

Method	H_2		H_3	
	KS	KS + SIC	KS	KS + SIC
B-P	0.7505		0.9361[b]	
B-PW	0.7481	0.7304	0.9343	0.9212
B-LPY	0.7468	0.7273	0.9360	0.9180
B3P	0.7443		0.9296	
B3PW	0.7445	0.7300	0.9297	0.9205
B3LYP	0.7430	0.7275	0.9300	0.9180
HF	0.734		0.933	
MP2	0.737		0.918	
CCSD(T)	0.742		0.930	
expt.	0.741			

[a] 6-311++G(*d*, 3*pd*) basis set was used in all calculations
[b] Equilibrium structure with no imaginary frequency

that the bond-shortening effect observed for LDA + SIC [27, 31] is also valid for GGA + SIC methods. It is interesting to note that the inclusion of the exact exchange influences the SIC geometries very slightly.

Frequency analysis shows that the B-P method provides no imaginary frequency for the H_3 $D_{\infty h}$ structure; thus it is qualitatively incorrect, while the B-PW method provides qualitatively correct results. Usually the B-P and B-PW functionals provide rather similar results; however, this is not true for H_3. Earlier results show [2] that the SIC considerably influences the vibrational frequencies for H_2 and H_3. The GGA-DFT methods underestimate the experimental frequency of H_2 by 65 cm^{-1}, while the inclusion of SIC overestimate the experimental frequency by about 300 cm^{-1} [2]. The GGA-DFT methods provide too small imaginary frequencies for H_3 $D_{\infty h}$ while the inclusion of the SIC provides considerably better agreement with CCSD(T) results.

The considerable bond shortening and the large frequency overestimation caused by the SIC for H_2 shows that the self-interaction error works similarly to the correlation effects and it contributes to the very good GGA results. The SIC has considerably greater effects than the inclusion of the exact exchange, the latter having a very small impact on GGA + SIC results. It can

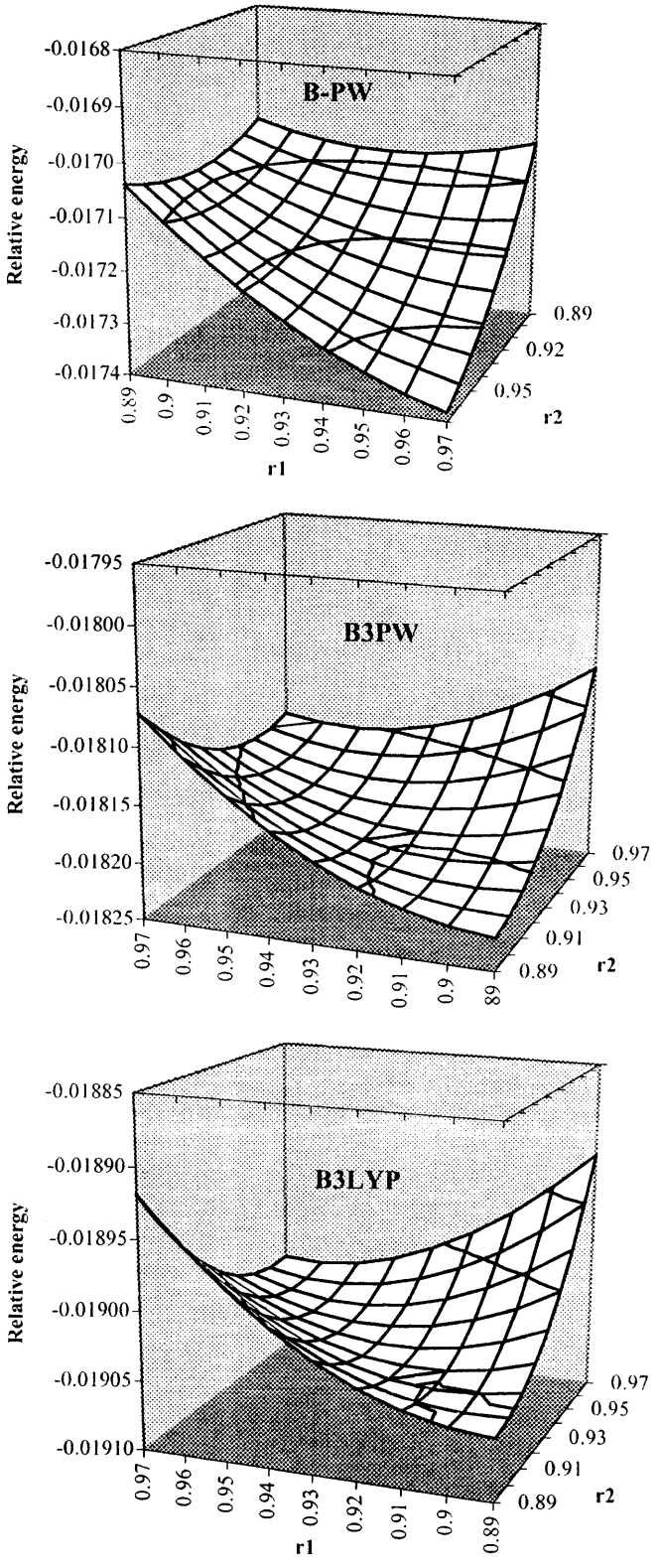

Fig. 1. Potential energy surface differences (a.u.) relative to CCSD(T) for H_3 $C_{\infty v}$ structure. r_1 and r_2 are the two internuclear distances (Å)

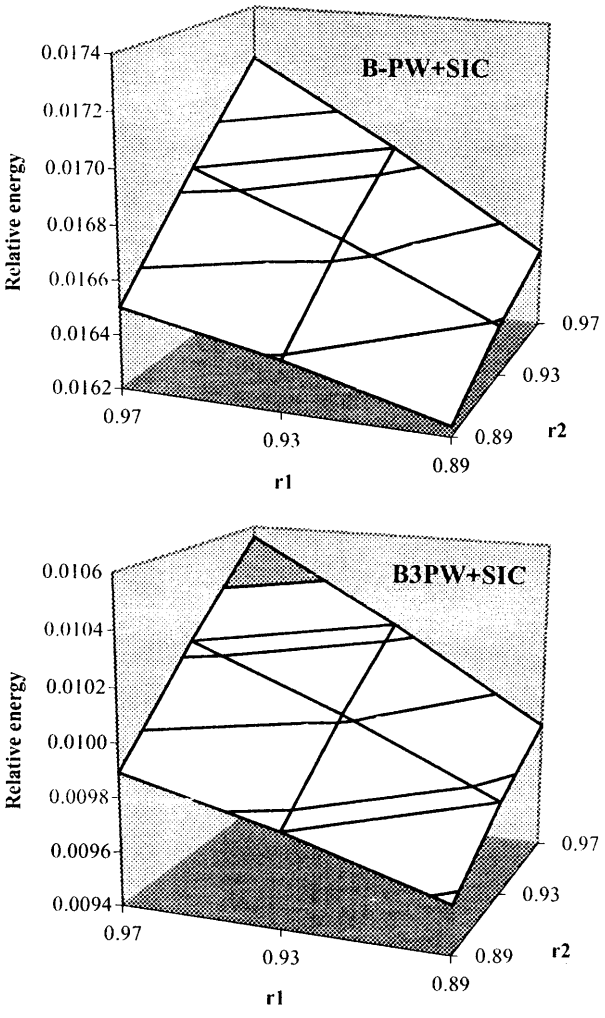

Fig. 2. KS + SIC potential energy surface differences (a.u.) relative to CCSD(T) for H_3 $C_{\infty v}$ structure. r_1 and r_2 are the two internuclear distances (Å)

be observed that self-interaction and the inclusion of the exact exchange work in the same direction (cf. Table 1).

3.2 Potential energy surfaces

We investigated the effects of the SIC and the inclusion of the exact exchange for the potential energy surface (PES) of H_3 around the transition state. The reference surface was calculated at the CCSD(T)/6-311++G(*d*,3*pd*) level of theory, which shows excellent agreement with experiment and very high level calculations. For example the transition state energy agrees with full-CI/6-311++G(*d*,3*pd*) energy within a microhartree [2]. Figure 1 shows the plots of PES differences between the selected and reference methods. The GGA-DFT results provide considerably lower energy than the CCSD(T) method. The B-LYP results, not shown in Fig. 1, are very close to the B-PW results. The inclusion of the exact exchange leads to further energy lowering and considerably flatter difference surface (the surface is nearly parallel with the CCSD(T) surface) in the symmetric stretching direction. The asymmetric stretching shows more important differences resulting a rather curved surface for B3PW and B3LYP methods in Fig. 1.

Figure 2 shows the effect of the inclusion of the SIC on the H_3 PES around the transition state. In contrast to the noncorrected GGA results, the GGA + SIC relative energy surfaces are higher in energy than the CCSD(T) surface. The self-interaction error yields an unphysical energy lowering that is quite common for GGA-DFT methods and even more pronounced for hybrid functionals. The SIC effectively corrects this error. The GGA + SIC and CCSD(T) PES differences are rather planar, but they have larger slopes than non-SIC DFT surfaces (cf. Figs. 1 and 2). It can be noted that the B3LYP + SIC surface agrees best with the CCSD(T) surface (not shown in Fig. 2). Another observation is that the inclusion of the SIC makes the four (B-PW, B-LYP, B3PW, and B3LYP PES) difference surfaces very similar, and inclusion of the exact exchange yields only a constant shift of the surface. Note that the B3 + SIC surfaces approximate the CCSD(T) surface better than the B + SIC surfaces (cf. Fig. 2).

3.3 Decomposition of the SIC

Table 2 shows the SIC energy correction terms for H_3 in the same distance range as shown in Figs. 1 and 2. These results show that the SIC is larger for the B-PW functional than for the B-LYP functional, and the inclusion of the exact exchange decreases the self-interaction error to 82% nearly uniformly.

Table 3 shows the SIC components in kcal/mol for H, H_2 and H_3. The imperfect cancellation of the Coulomb term (E_J) by the corresponding exchange term (E_X) yields less than 1 kcal/mol self-interaction error for H and H_2 if the pure Becke exchange functional is used; however, the inclusion of the exact exchange and the Slater term together makes this error 3 times larger for H and 6–12 times larger for H_2. This is because the inclusion of the exact exchange and the Slater term increases the positive Coulomb term only slightly and results in a

Table 2. The SIC energy correction (kcal/mol) for H_3 at various internuclear distances (Å)[a]

r_1	r_2	B-PW	B3PW	B-LYP	B3LYP
0.89	0.89	20.62	17.13	8.17	6.76
0.89	0.93	20.75	17.22	8.36	6.90
0.89	0.97	20.80	17.24	8.48	6.98
0.93	0.93	21.00	17.39	8.67	7.13
0.93	0.97	21.17	17.50	8.91	7.29
0.97	0.97	21.45	17.70	9.26	7.55

[a] 6-311++G(*d*, 3*pd*) basis set was used in all calculations

Table 3. The KS + SIC H_2 equilibrium, and H_3 $D_{\infty h}$ transition structures (Å) and SIC energy components (kcal/mol) for H, H_2 and H_3 calculated with various methods

	$R_{(H\text{-}H)}$	E_J	E_X	$E_J + E_X$	E_{Crr}	E_{SIC}
B-PW + SIC						
H.		193.67	−192.61	1.07	−4.06	2.99
H_2	0.7304	416.24	−415.35	0.88	−9.14	8.26
H_3	0.9212	575.44	−583.03	−7.59	−13.25	20.83
B3PW + SIC						
H.		193.99	−190.91	3.09	−5.96	2.88
H_2	0.7300	416.44	−410.93	5.51	−12.95	7.45
H_3	0.9205	577.45	−575.96	1.49	−18.81	17.33
B-LYP + SIC						
H.				0.86	0.00	−0.86
H_2	0.7273	415.00	−414.61	0.38	0.00	−0.38
H_3	0.9180	574.79	−583.30	−8.51	0.00	8.51
B3LYP + SIC						
H.		193.27	−190.31	2.96	−2.62	−0.34
H_2	0.7275	415.56	−410.35	5.20	−5.45	0.24
H_3	0.9180	576.94	−576.02	0.92	−7.93	7.01

[a] 6-311++G(*d*,3*pd*) basis set was used in all calculations

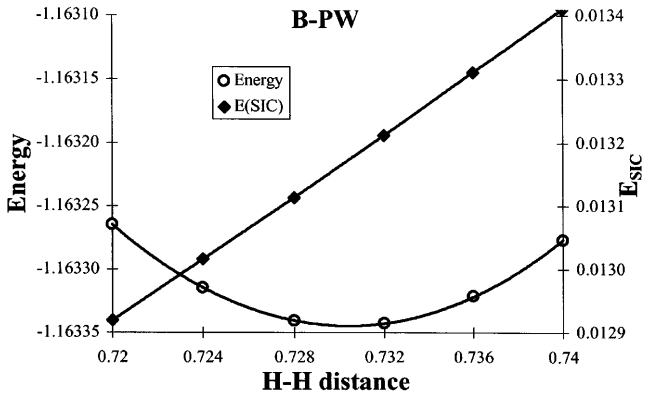

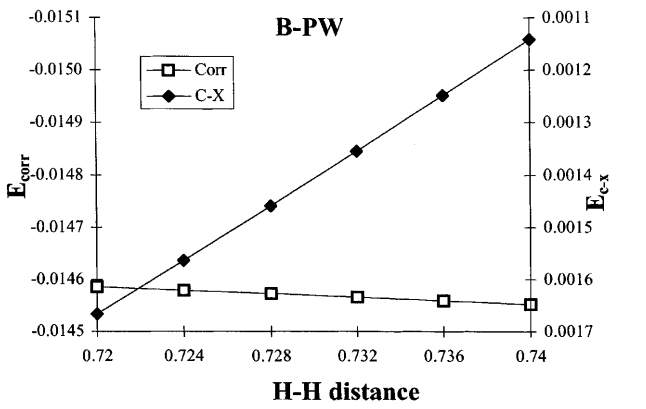

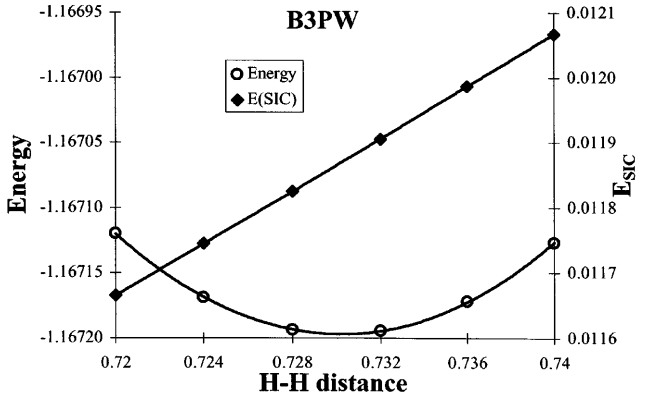

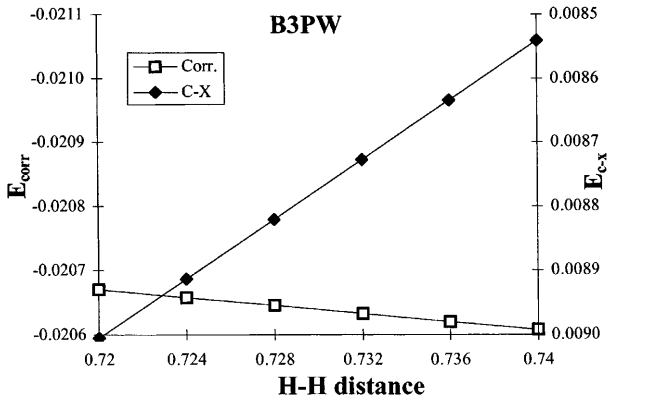

Fig. 3. Potential energy and SIC curves (a.u.) for H_2 as a function of internuclear distance (Å). The SIC curves are decomposed to Coulomb exchange ($E_{C\text{-}X}$) and correlation (*Corr.*) components on the *right*

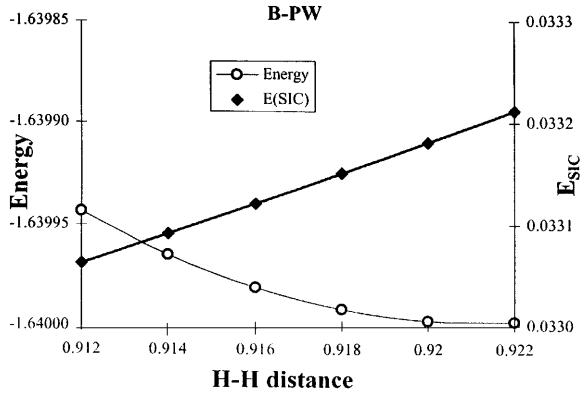

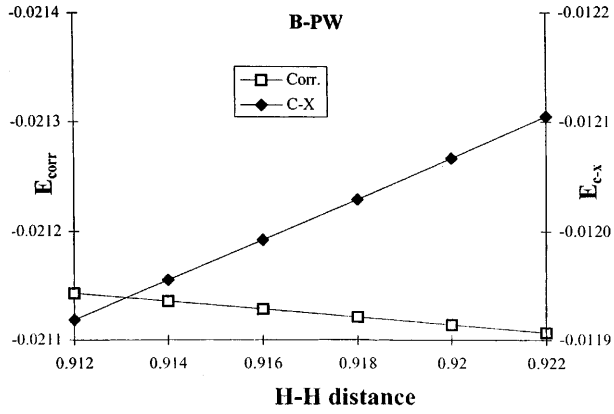

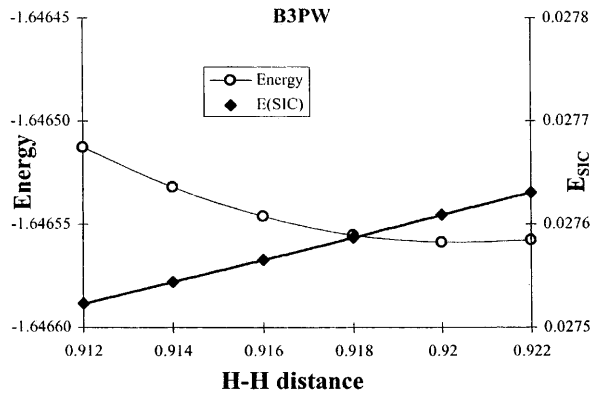

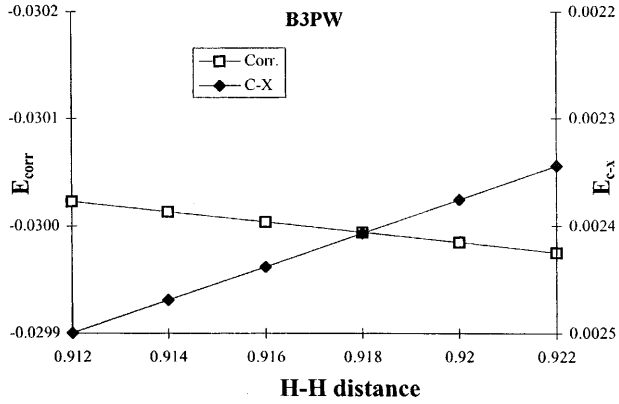

Fig. 4. Potential energy and SIC curves (a.u.) for H_3 $C_{\infty h}$ structure as a function of internuclear distance (Å). The SIC curves are decomposed to Coulomb exchange ($E_{C\text{-}X}$) and correlation (*Corr.*) components on the *right*

more important increase in the negative exchange term. Thus the inclusion of the exact exchange and the Slater term changes the existing, slightly positive balance of the Becke functional in a positive direction. For H_3 the situation is essentially different as the pure Becke functional provides a large negative value for $E_J + E_X$. The inclusion of the exact exchange increases the negative exchange term by about 9 kcal/mol, thus helping to obtain a considerably better balance (Table 3).

Investigation of the correlation terms in Table 3 shows that the correlation functional mixing proposed by Becke [18] increases the self-interaction error uniformly. This is because the large self-interaction error of the LSDA exchange correlation functional becomes more dominant in the hybrid formalism than in the GGA formalism. This can be seen clearly in Table 3, where the zero self-interaction error of the LYP correlation functional becomes nonzero in the hybrid correlation functional. In the B-LYP functional the origin of the self-interaction error is purely the self-interaction error of the Becke's exchange functional because, as noted earlier, the LYP functional has no self-interaction error. The results in Table 3 show that the self-interaction error of the B exchange and the PW correlation functional has the opposite sign. The origin of the relatively large self-interaction error of the B-PW functional is that the correlation self-interaction error largely overcompensates the exchange self interaction error. It is important to note that the correlation SIC energy components increase with the size of the system and the correlation SIC for H_3 is nearly equal to the sum of the correlation SIC for H and H_2 (cf. Table 3). As a consequence the correlation self-interaction error practically disappears from the barrier error. Thus the source of the error of the barrier is the self-interaction error of the exchange functional. Our results show that the exact exchange mixing does not provide a size-extensive, uniform improvement (Table 3). Further efforts are required essentially on the exchange side in order to eliminate the self-interaction error from the hydrogen abstraction barriers. In this sense the use of the self-interaction free exact exchange [32, 33] provides a promising solution.

Figure 3 shows the potential energy and SIC curves for H_2. Figure 4 illustrates the symmetric stretching and SIC curves for the H_3 $D_{\infty h}$ structure. The figures clearly shows that the error in the Coulomb exchange balance term dominates in the SIC curve. Qualitatively similar curves were obtained for the B-LYP (not shown here) and B-PW functionals.

3.4 Barrier height

The total energies for H, H_2 and H_3 involved in the reaction, and the classical barrier heights obtained with the investigated DFT methods are shown in Table 4. For reference purposes, we show the MP2 and CCSD(T) barriers and a high-quality quantum Monte Carlo (QMC) result [42]. The latter method results in 9.61 kcal/mol for the barrier height, which is very close to the experimental value of 9.7 kcal/mol [43]. The KS results provide too low reaction barrier. The B3 methods are about 1 kcal/mol closer to the experiment. The inclusion of the SIC increases the B-XX energies by more than 9.5 kcal/mol, and it increases the B3 energies by about 7 kcal/mol. Thus the B3 + SIC methods provide better energies than the B + SIC methods. The best agreements with the experimental barrier height were provided by self-interaction corrected B3LYP, B-LYP and B3PW methods with errors of 1.5, 2.9 and 3.0 kcal/mol, respectively (the noncorrected B3LYP error was about –5.5 kcal/mol) (cf. Table 4).

4 Conclusions

The pure GGA and especially the hybrid methods yield an excellent H_2 equilibrium bond length, while inclusion of the SIC yields results in a H_2 bond distance that is too short (even shorter than that of the HF method). The inclusion of the SIC results in a rather large, 300 cm^{-1} overestimation of the H_2 vibrational frequency. However, for the H_3 imaginary frequency the GGA + SIC results show considerably better agreement with the CCSD(T) results than the uncorrected GGA or hybrid results. The self-interaction error results in an electron correlation-like effect (bond lengthening, frequency shift); thus it contributes to the good results of the uncorrected GGA calculations.

Table 4. Calculated total energies (au) of H, H_2, and H_3 and classical barrier height (kcal/mol) of $H + H_2 \rightarrow H_3$ reaction[a]

Method	H		H_2		H_3		Classical barrier height[b]	
	KS	KS + SIC	KS	KS + SIC	KS	KS + SIC	KS	KS + SIC
B-PW	−0.50416	−0.49939	−1.17673	−1.16334	−1.67335	−1.64000	4.73	14.26
B3PW	−0.50417	−0.49958	−1.17923	−1.16720	−1.67430	−1.64656	5.71	12.69
B-LYP	−0.49772	−0.49909	−1.16962	−1.16998	−1.66279	−1.64904	2.86	12.57
B3LYP	−0.49887	−0.49941	−1.17331	−1.17272	−1.66568	−1.65442	4.08	11.11
MP2	−0.49982		−1.16495		−1.64372		13.21	
CCSD(T)	−0.49982		−1.17253		−1.65652		9.91	
QMC[c]							9.613	
Expt.[d]							9.7	

[a] 6-311++G(*d*,3*pd*) basis set and the geomeries shown in Table 1 were used in all calculations
[b] Zero-point corrections for KS, KS + SIC, and CCSD(T) are −0.69, −0.96 and −0.83 kcal/mol. respectively; see [2]
[c] From [42] the error is ±0.006 kcal/mol
[d] From [43]

Comparison of the CCSD(T) energy surface with various GGA, hybrid and GGA + SIC surfaces around the H_3 $D_{\infty h}$ transition state shows that the SIC plays a very important role; thus it makes the unphysical energy lowering disappear. The B3LYP + SIC surface agrees best with the CCSD(T) surface and this method provides the best barrier height. The inclusion of the exact exchange results in a constant shift of the energy surface. The hybrid functionals show only a slight improvement for the hydrogen abstraction barrier compared to the pure GGA-DFT functionals.

The improvements provided by the inclusion of the SIC are the following: it corrects the unphysical low energies present in various GGA functionals; it provides a good hydrogen abstraction barrier and a good H_3 imaginary frequency (thus good curvature around the transition state). However, the inclusion of the SIC for GGA results in poor molecular geometry and bonding vibrational frequencies.

The exchange functional mixing proposed by Becke increases the Coulomb exchange part of the self-interaction error for H and H_2 and decreases it for H_3. Formally the hybrid functional provides lower SIC energy; however, the better results originate simply from the larger errors in the exchange part for H and H_2 that compensate the correlation self-interaction errors better. For H_3 the situation is different; the hybrid method results in a considerably smaller self-interaction error for the exchange. The correlation functional mixing proposed by Becke increases the self-interaction error uniformly and considerably; however, the errors arising from this factor cancel each other out for the H_3 energy barrier. The principal source of the barrier error is the self-interaction error of the Coulomb exchange term; thus the self-interaction free exchange functional should be used to solve this problem.

Acknowledgements. We are grateful to Prof. John P. Perdew for helpful discussions and for reading the manuscript. G.I.C. acknowledges the PAST professorship provided by the French Government, and the kind hospitality of Prof. J.-L. Rivail and Dr. B. Maigret. The financial support of the Hungarian Research Foundation (OTKA T14247, and T16328) is acknowledged.

References

1. Partridge H, Bauschlicher CW Jr, Stallcop JR, Levin E (1993) J Chem Phys 99: 5951
2. Johnson BG, Gonzales CA, Gill PMW, Pople JA (1994) Chem Phys Lett 221: 100, and references cited therein
3. Boothroyd AI, Keogh WJ, Martin PG, Peterson MR (1996) J Chem Phys 104: 7139, and electronic files for H_3 potential energy surface via anonymous ftp://ftp.cita.utoronto.ca/cita/pgmartin/h3pes/readme
4. Warnatz J (1984) In: Gardiner WC Jr (ed) Combustion chemistry. Springer, Berlin Heidelberg New York
5. Hucknall DJ (1985) In: Chemistry of hydrocarbons. Chapman and Hall, London
6. Gonzalez C, MacDouall JJM, Schlegel HB (1990) J Chem Phys 94: 7467
7. Shatz GC, Wagner AF, Dunning TH Jr (1984) J Phys Chem 88: 221
8. Kreevoy MM, Truhlar DG (1986) In: Bernasconi CF (ed) Investigation of rates and mechanisms of reactions. Wiley, New York, and references cited therein
9. Kohn W, Sham L (1965) J Phys Rev A140: 1133
10. Perdew JP, Parr RG, Levy M, Balduz JL Jr (1982) Phys Rev Lett 46: 1691
11. Ernzerhof M, Perdew JP, Burke K (1996) In: Nalewajski RF (ed) Density functional theory. Topics in current chemistry. Springer, Berlin Heidelberg New York, pp 3
12. (a) Perdew JP, Wang Y (1986) Phys Rev B 33: 8800; (b) Perdew JP (1986) Phys Rev B 33: 8822
13. Becke AD (1986) J Chem Phys 84: 4524
14. Becke AD (1988) Phys Rev A 38: 3098
15. Lee C, Yang W, Parr RG (1988) Phys Rev B 37: 785
16. Becke AD (1992) J Chem Phys 96: 2155, J Chem Phys (1992) 97: 9173
17. Langreth DC, Perdew JP (1977) Phys Rev B 15: 2884, and references cited therein
18. Becke AD (1993) J Chem Phys 98: 5648
19. Becke AD (1996) J Chem Phys 104: 1040
20. Baker J, Muir M, Andzelm J (1995) J Chem Phys 102: 2063
21. Baker J, Andzelm J, Muir M, Taylor PR (1995) Chem Phys Lett 237: 53
22. Perdew JP, Zunger A (1981) Phys Rev B 23: 5048, and references cited therein
23. Perdew JP (1990) In: Trickey SB (ed) Density functional theory of many-fermion systems. Advances in quantum chemistry, vol 21. Academic Press, New York
24. Li Y, Krieger JB (1990) Phys Rev A 41: 1701
25. Lindgen I (1971) Int J Quantum Chem 4: 411
26. Chen J, Krieger JB, Li Y, Iafrate GJ (1996) Phys Rev A 54: 3939, and references therein
27. Groedecker S, Umringar C (1997) Phys Rev A 55: 1765
28. Norman MR (1983) Phys Rev B 28: 3585
29. Penderson MR, Heaton RA, Harrison JG (1989) Phys Rev b 39: 1581
30. Perdew JP (1985) In: Dreizler RM, da Providencia J (eds) Density functional methods in physics. Plenum Press, New York
31. Krieger JB, Chen J, Iafrate JG (1996) Bull Am Phys Soc 41: 748, abstracts R19 11–12
32. Krieger JB, Li Y, Iafrate JG (1992) Phys Rev A 45: 101
33. Perdew JP, Ernzerhof M (1997) In: Dobson JF, Vignale G, Das MP (eds) Electronic density functional theory: recent progress and new directions. Plenum Press, New York
34. Grabo T, Gross EKU (1995) Chem Phys Lett 240: 141
35. Colle R, Salvetti D (1975) Theor Chim Acta 37: 329
36. Colle R, Salvetti D (1979) Theor Chim Acta 53: 55
37. (a)Perdew JP (1991) In: Ziesche P, Eschrig H (eds) Electronic structure of solids '91. Akademie Verlag, Berlin, p 11; (b) Perdew JP, Burke K, Wang Y (1996) Phys Rev B 54: 16533
38. Vosko SH, Wilk L, Nussair M (1980) Can J Phys 58: 1200
39. Frisch MJ, Trucks GW, Head-Gordon M, Gill PMW, Wong MW, Foresman JB, Johnson BG, Schlegel HB, Robb MA, Replogle ES, Gomperts R, Andres JL, Raghavachari JS, Binkley JS, Gonzalez C, Martin RL, Fox DJ, DeFrees DJ, Baker J, Stewart JJP, Pople JA (1995) Gaussian 94, Revision B. Gaussian, Pittsburgh, Pa
40. Q-Chem Inc., 317 Whipple Street, Pittsburgh, PA 15218, USA
41. Hehre WJ, Radom L, Schleyer PvR, Pople JA (1986) Ab initio molecular orbital theory. Wiley, New York, and references cited therein
42. Dietrich DL, Anderson J (1992) Science 258: 786
43. Schultz WR, Leroy DJ (1965) J Chem Phys 42: 3869